Electronic Supplementary Material (ESI) for Journal of Materials Chemistry A.

In situ moulded Troilite 2H phase Fe S ultrathin electrodes via Pulsed Laser Deposition for Flexible Solid State High Capacity Supercapacitor besides boosted electrocatalytic oxygen evolution reaction

Ramasamy Velmurugan[a,b,#], Dekshinamoorthy Amuthan[a,b,#], Vijayaraghavan Saranyan[a,b*], Balasubramanian Subramanian[a,b,*]

[a]CSIR- Central Electrochemical Research Institute, Karaikudi- 630 003, Tamil Nadu, India.

[b]Academy of Scientific and Innovative Research (AcSIR), Ghaziabad- 201 002, India.

[#] Authors contributed equally

***Corresponding Author:** saranyan@cecri.res.in (Vijayaraghavan Saranyan), bsmanian@cecri.res.in (Balasubramanian Subramanian)

Formulae for Evaluation of capacitances, capacities, energy and power densities

Areal and Volumetric capacitances with respect to Scan rates

$$C_{(A)} = \frac{i\oint dV}{A\vartheta\Delta V}\left(\frac{mF}{cm^2}\right) \quad \text{-------------- (1)}$$

$$C_{(V)} = \frac{i\oint dV}{V\vartheta\Delta V}\left(\frac{F}{cm^3}\right) \quad \text{------------- (2)}$$

Areal and Volumetric capacitances with respect to Current density rates

$$C_{(Areal)} = \frac{I\oint dt}{A\Delta V}\left(\frac{mF}{cm^2}\right) \quad \text{----------- (3)}$$

$$C_{(Vol)} = \frac{I\oint dt}{V\Delta V}\left(\frac{F}{cm^3}\right) \text{ -------------- (4)}$$

Volumetric capacity with respect to Current density rates

$$C_{sp.v.}C_{cap} = \frac{i * dt}{3.6V}\left(\frac{mAh}{cm^3}\right) \text{ ----------- (5)}$$

Volumetric specific Energy

$$E_V = \frac{C_{DV}}{3.6}\left(\frac{mWh}{cm^3}\right) \text{ ------------- (6)}$$

Volumetric specific Power

$$P_V = \frac{E}{dt} \times 3.6 \left(\frac{W}{cm^3}\right) \text{ --------- (7)}$$

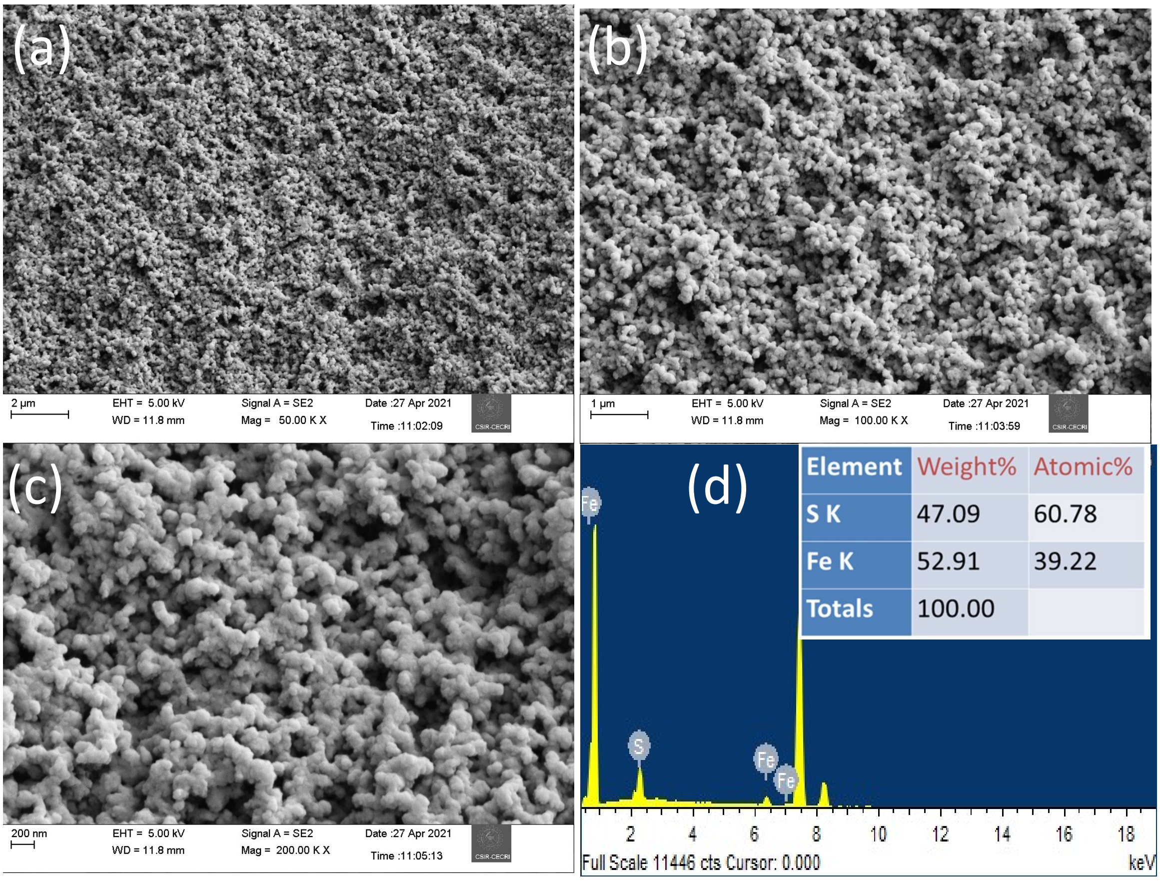

Figure S1: (a-c) FESEM morphologies of FeS thin film RT; (d) EDAX spectrum of FeS thin film RT

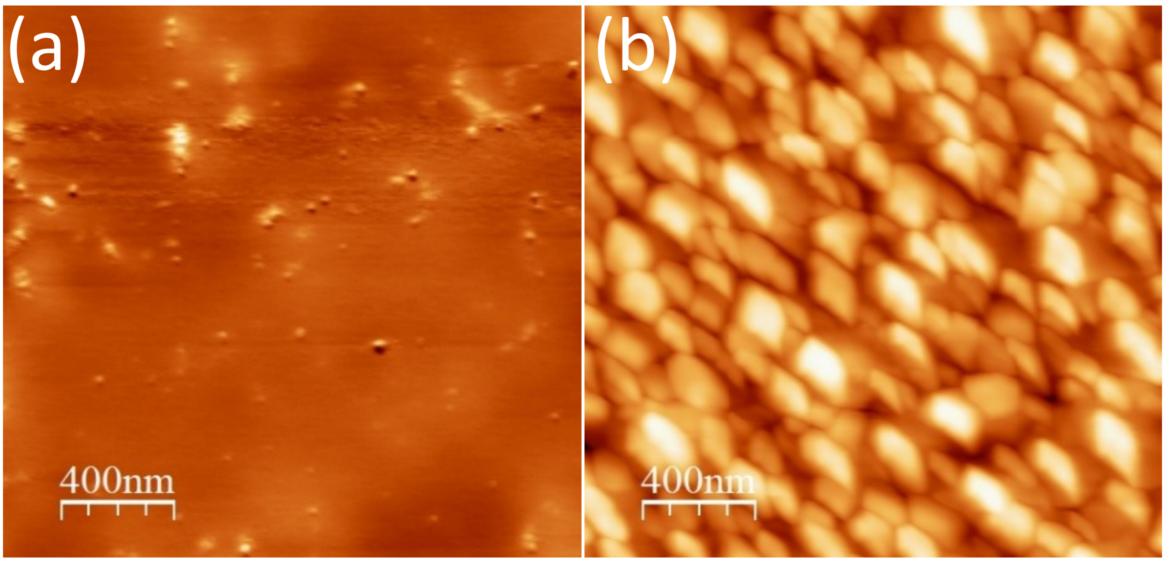

Figure S2: AFM 2D and 3D topographical images of FeS thin films RT and A650.

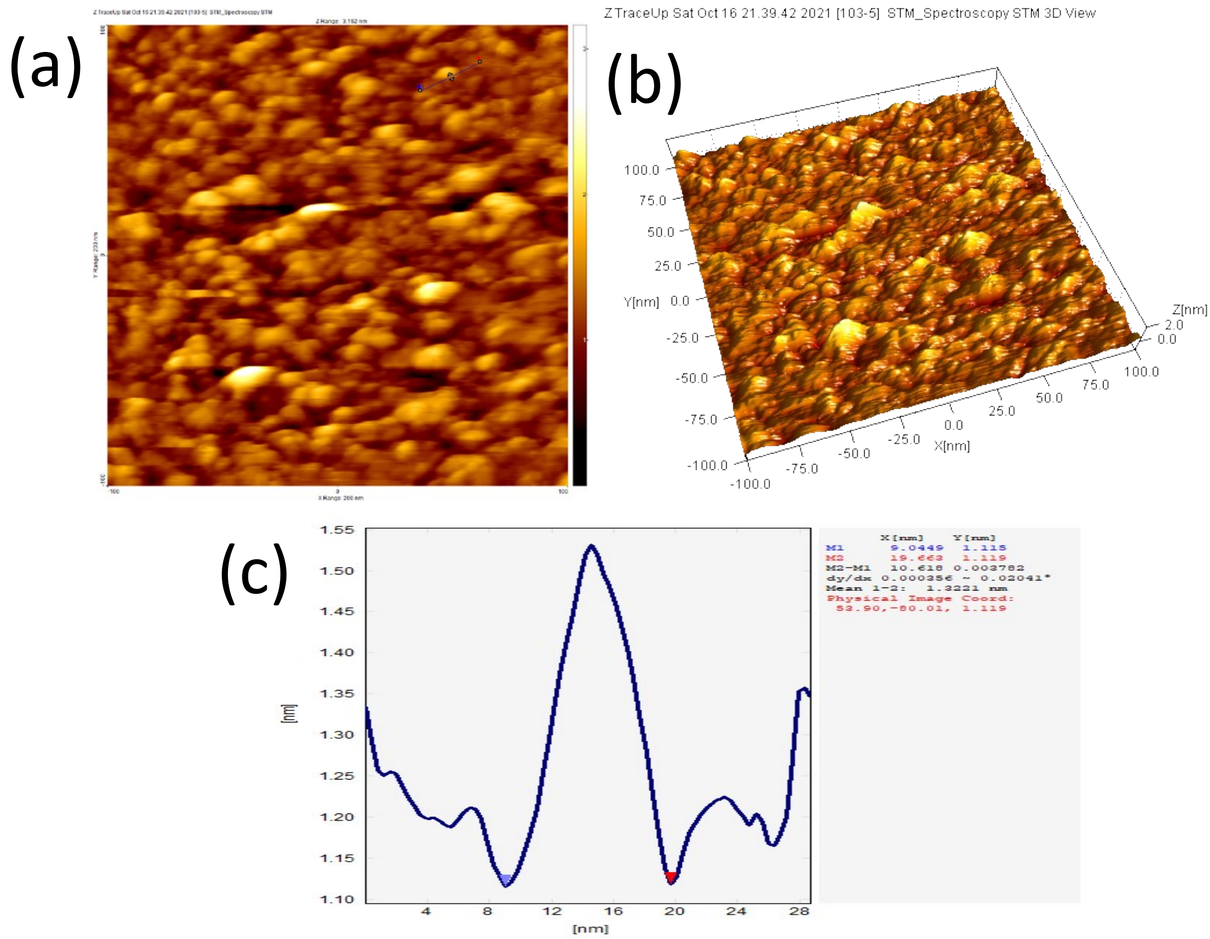

Figure S3 :(a& b) STM 2D and 3D atomic resolution images; (c) surface profile.

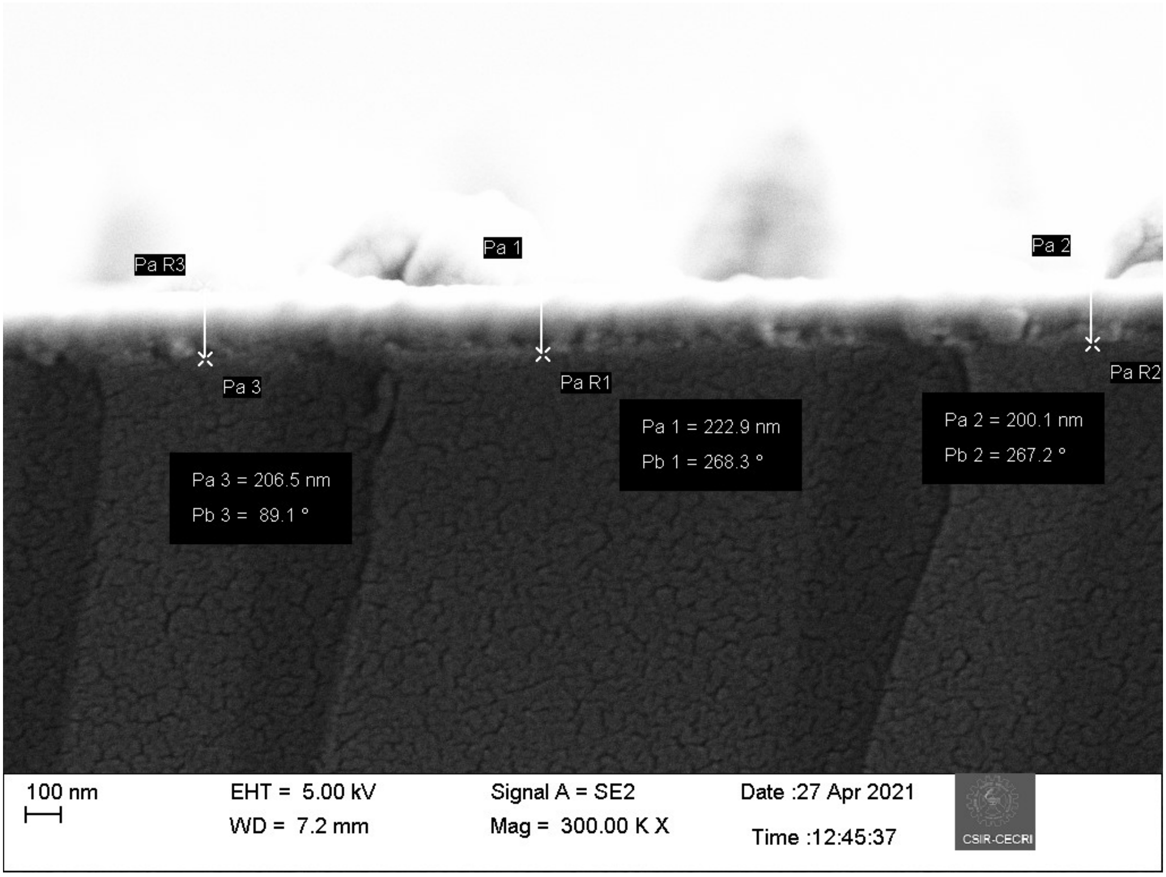

Figure S4: FESEM cross sectional image.

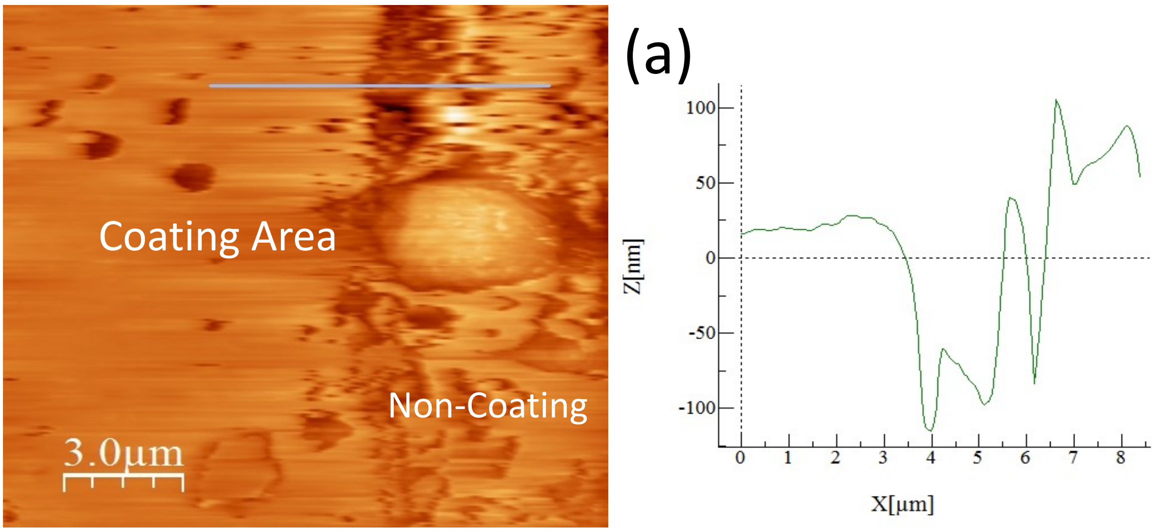

Figure S5: (a) AFM 2D topographical images of cross section measurement; (b) Thickness profile.

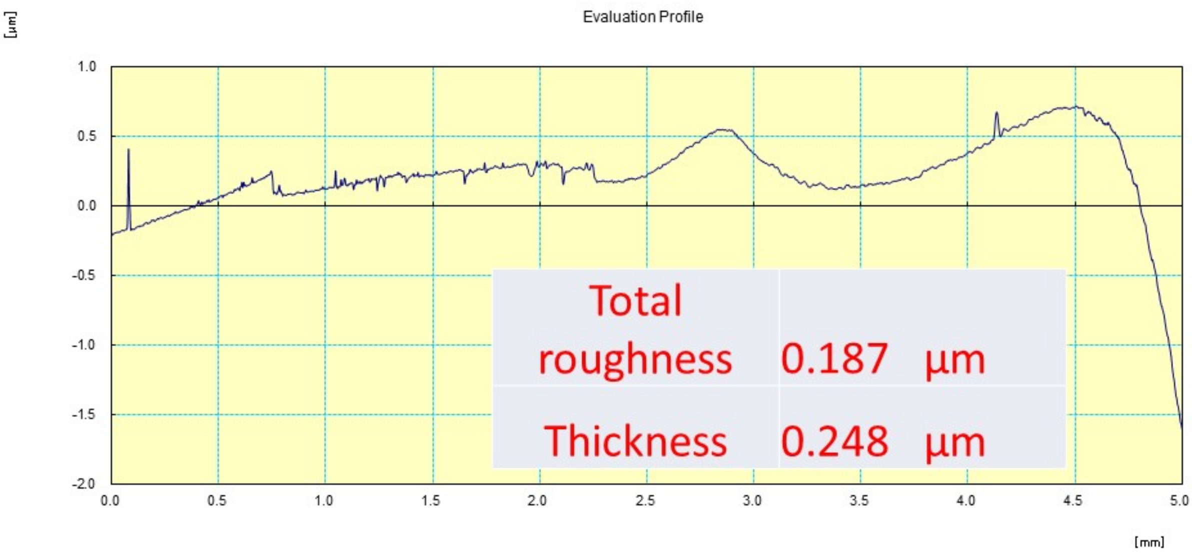

Figure S6: Thickness profilometer profile.

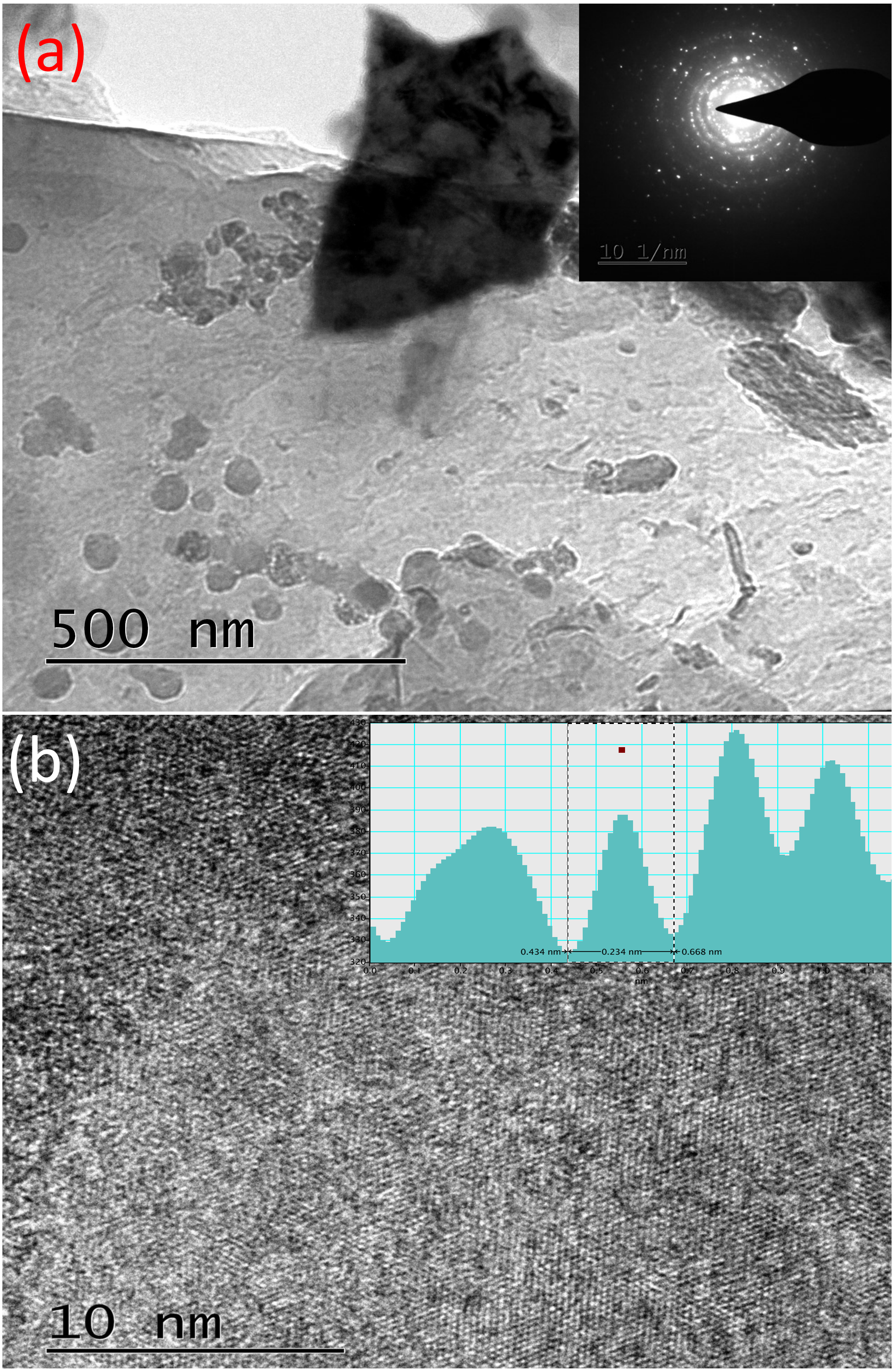

Figure S7: (a) TEM morphology of FeS RT (inset: SAED); (b) lattice fringes (inset: d-space profile).

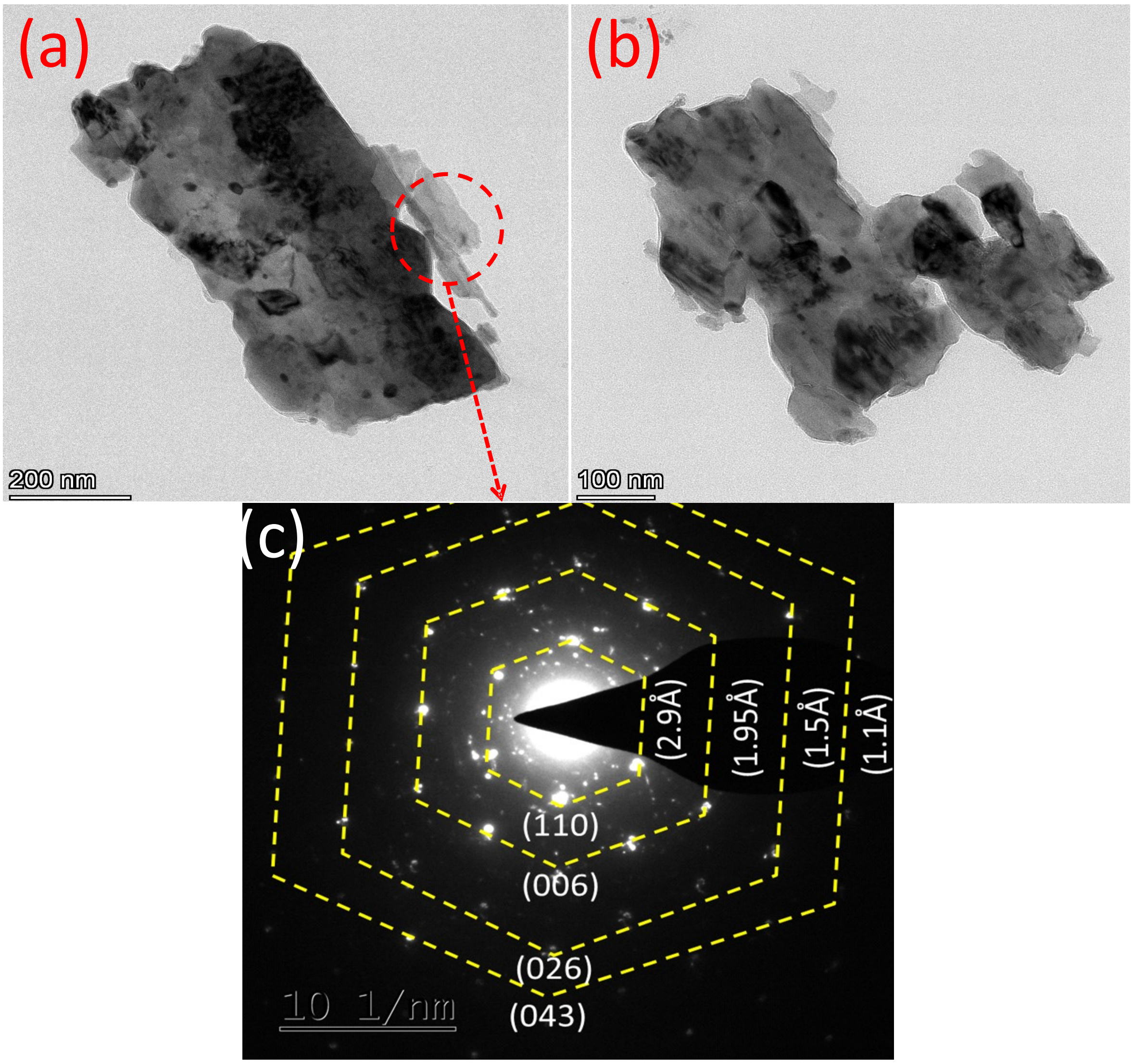

Figure S8: (a) Selected SAED area of TEM image of FeS A650 nano particles; (b) TEM image of FeS A650 other selected area; (c) SAED pattern of FeS A650 nano particles.

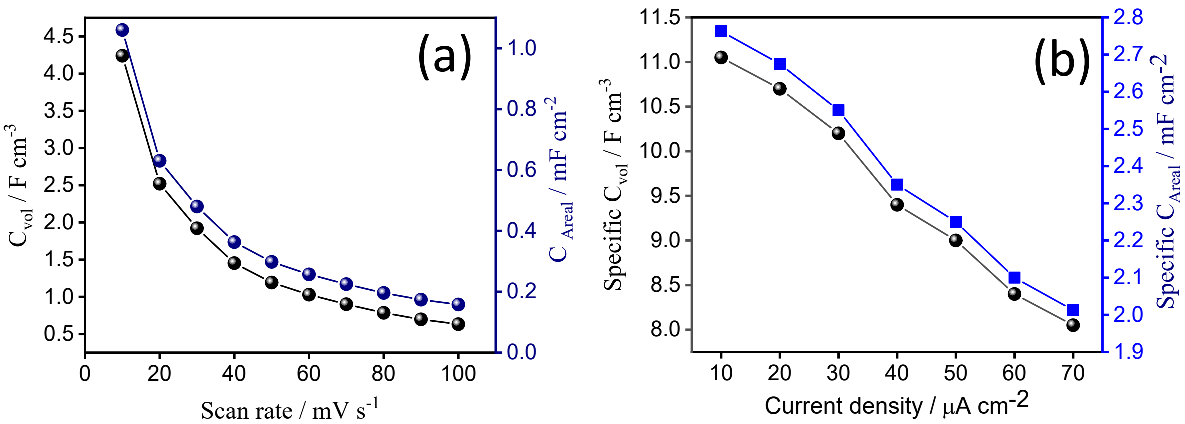

Figure S9: (a) Specific areal capacitance & Volumetric capacitance vs sweep rate of FeS thin film electrode RT; (b)Specific discharge areal capacitance & volumetric capacitance vs current rate of FeS thin film electrode RT.

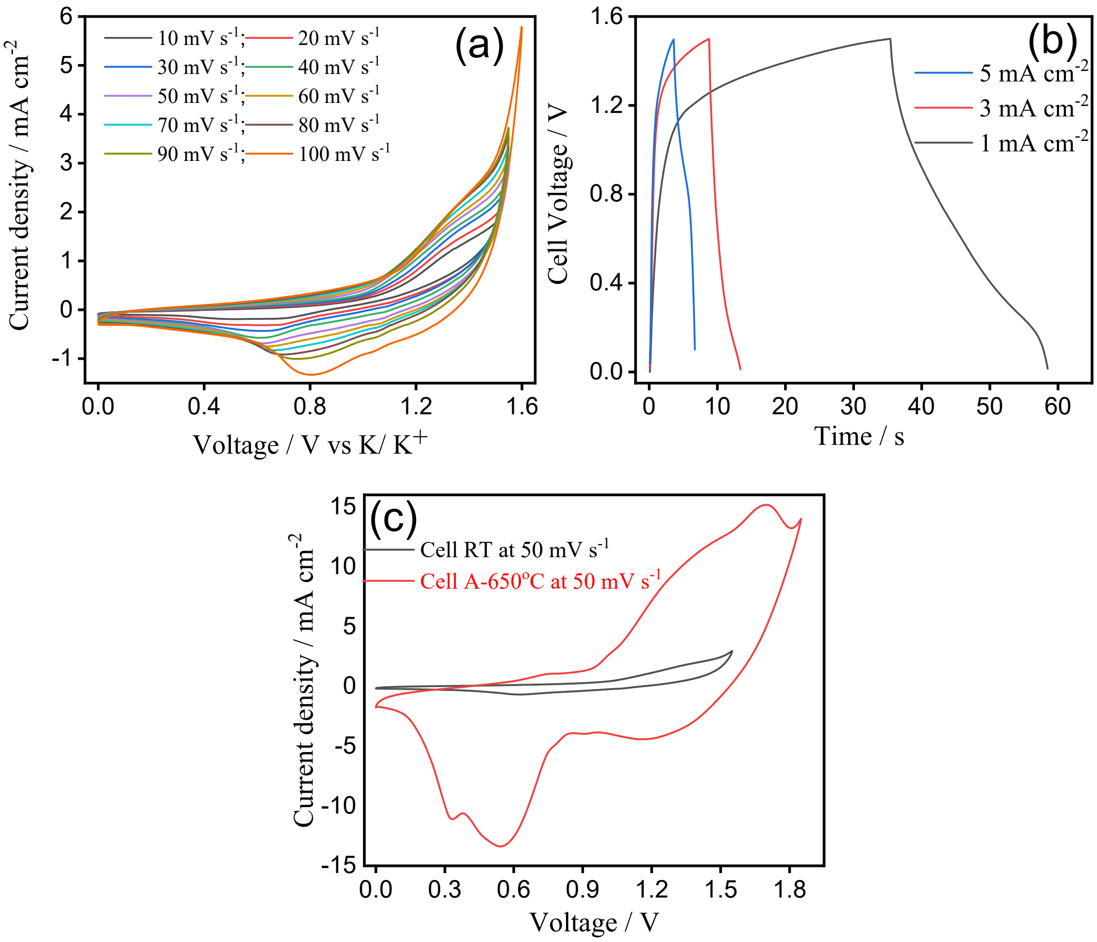

Figure S10: Electrochemical analysis of full cell (RT) (a) CV profile of FeS thin film symmetric device (RT) at scan rate of 10 to 100 mV s^{-1}; (b) GCD profile of FeS thin film symmetric device (RT) at varying current density range; (c) CV profile comparison for FeS thin film symmetric devices RT and cell-A650 at a scan rate 50 mV s^{-1}.

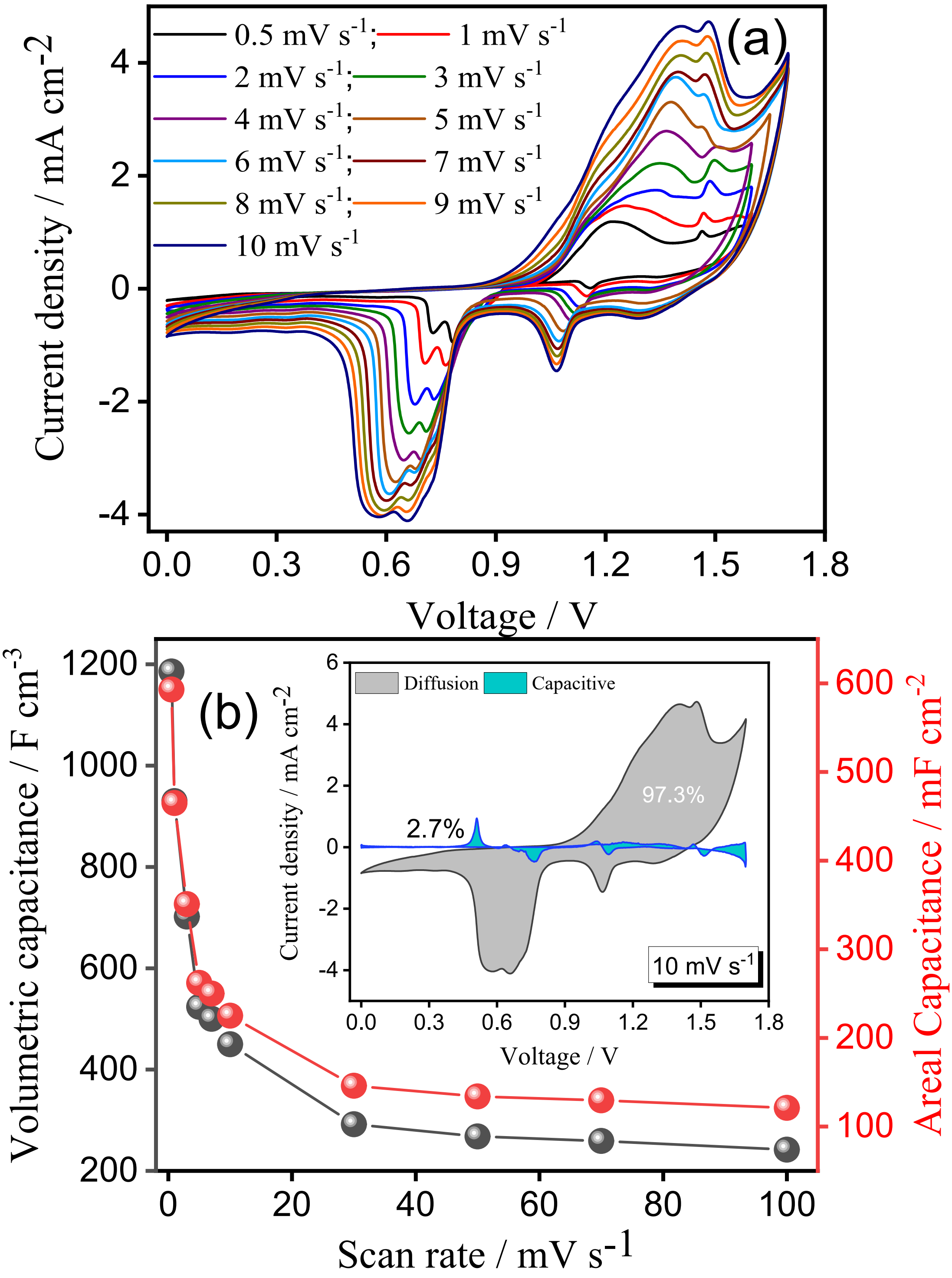

Figure S11: (a) CV curve of FeS symmetric device (A650) at low scan rates (0.5 to 10 mVs^{-1}); (b) Specific volumetric capacitance and areal capacitance vs scan rate.

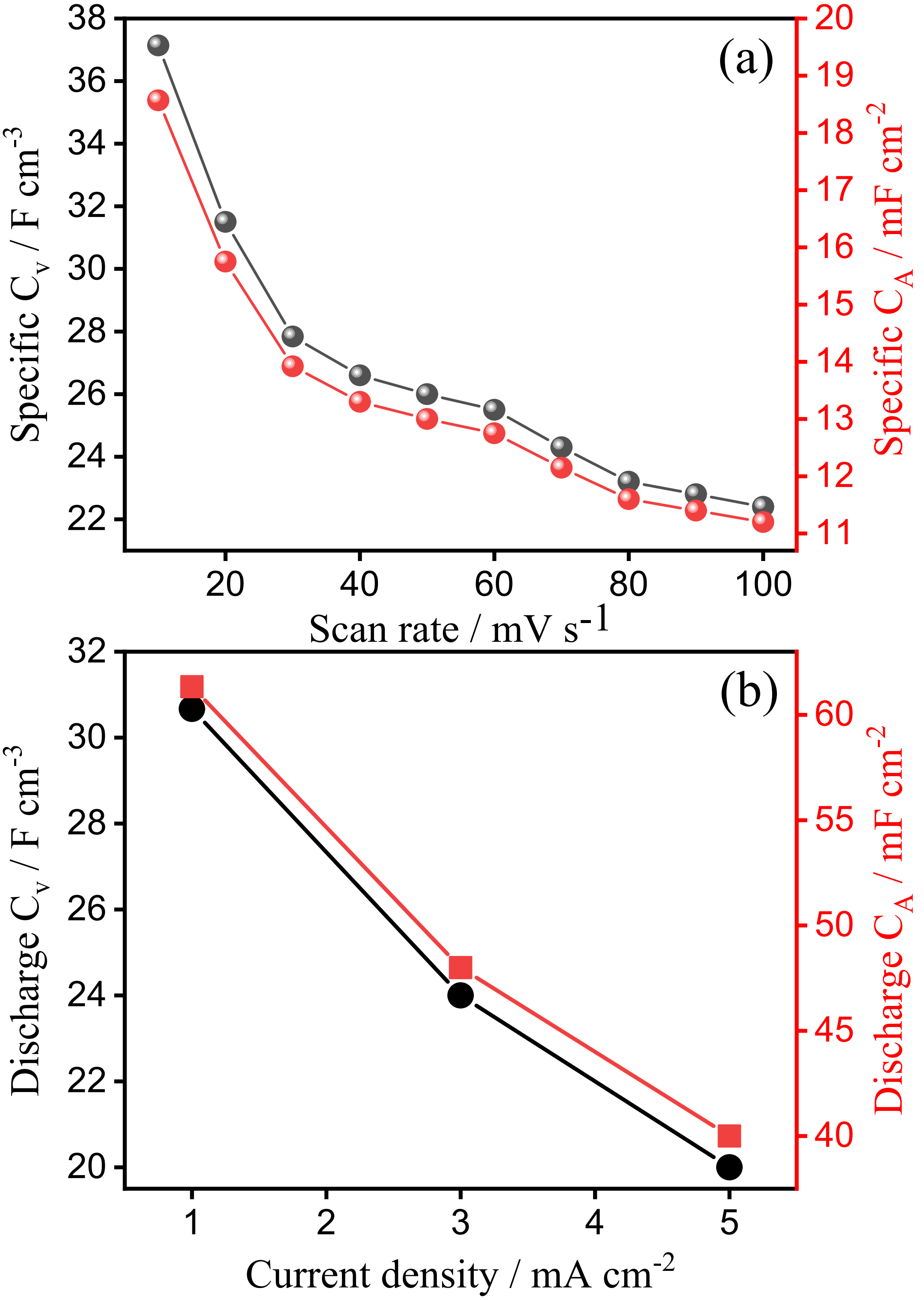

Figure S12: Electrochemical characterization of FeS Symmetric device RT (a) Specific volumetric and areal capacitance vs scan rate; (b) Specific volumetric capacitance vs current density.

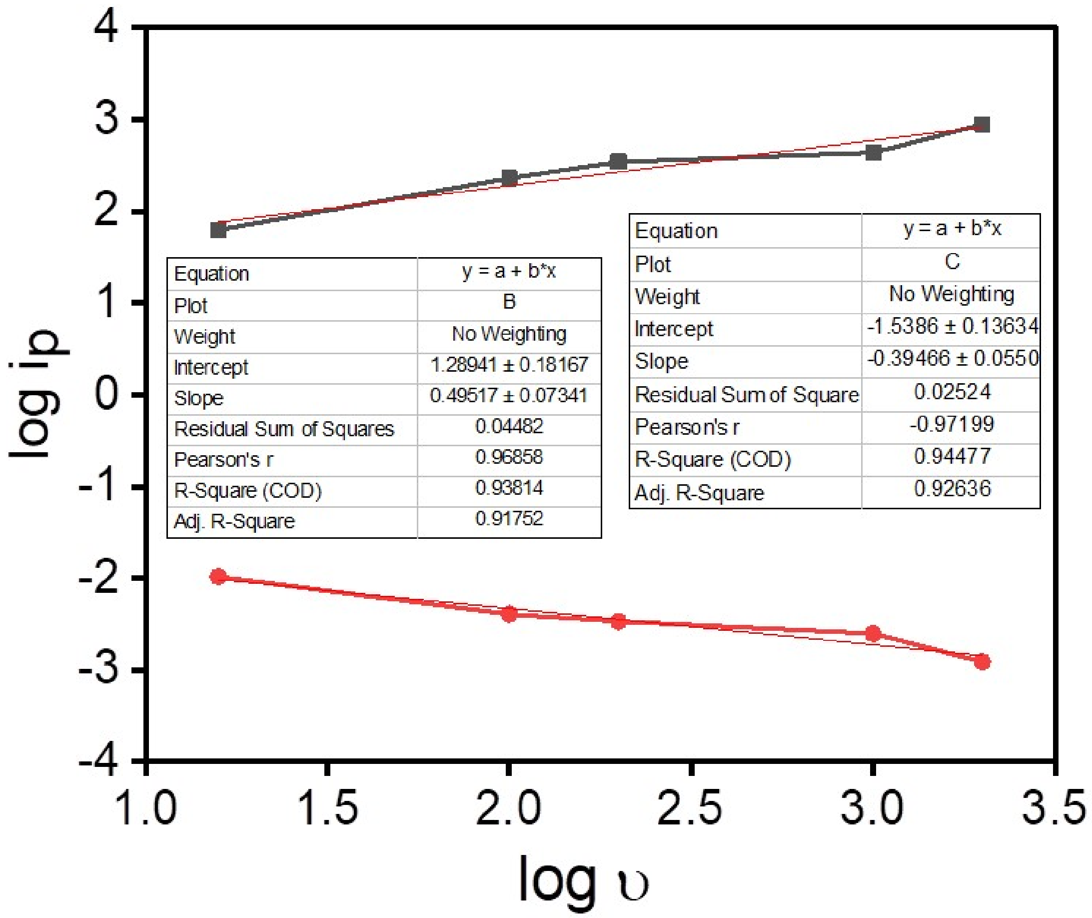

Figure S13: Slope (scan rare vs peak current) measurement curve from CV curve of FeS cell A650.

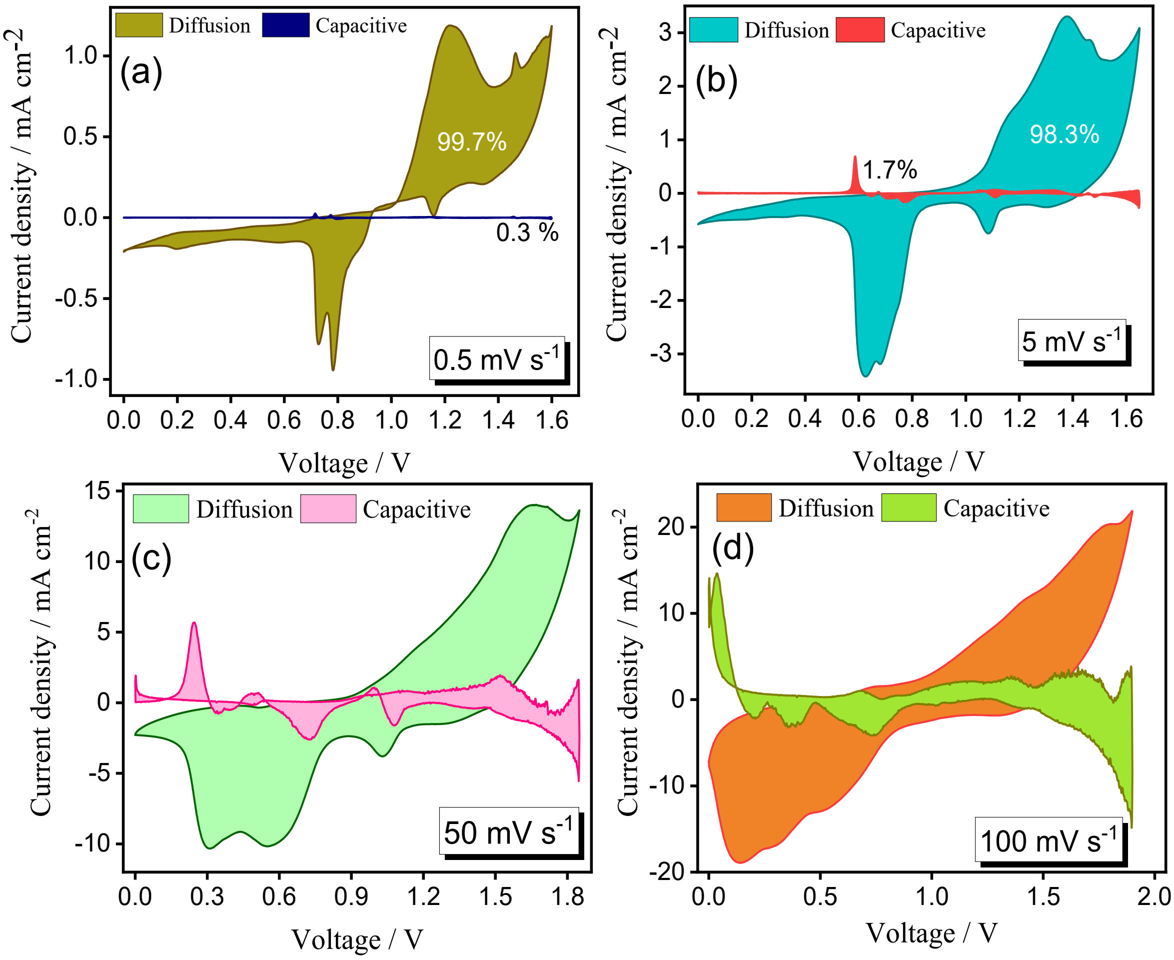

Figure S14: (a-d) CV curve comparison of contribution of diffusion and capacitive at 0.5, 5, 50 and 100 mVs^{-1}.

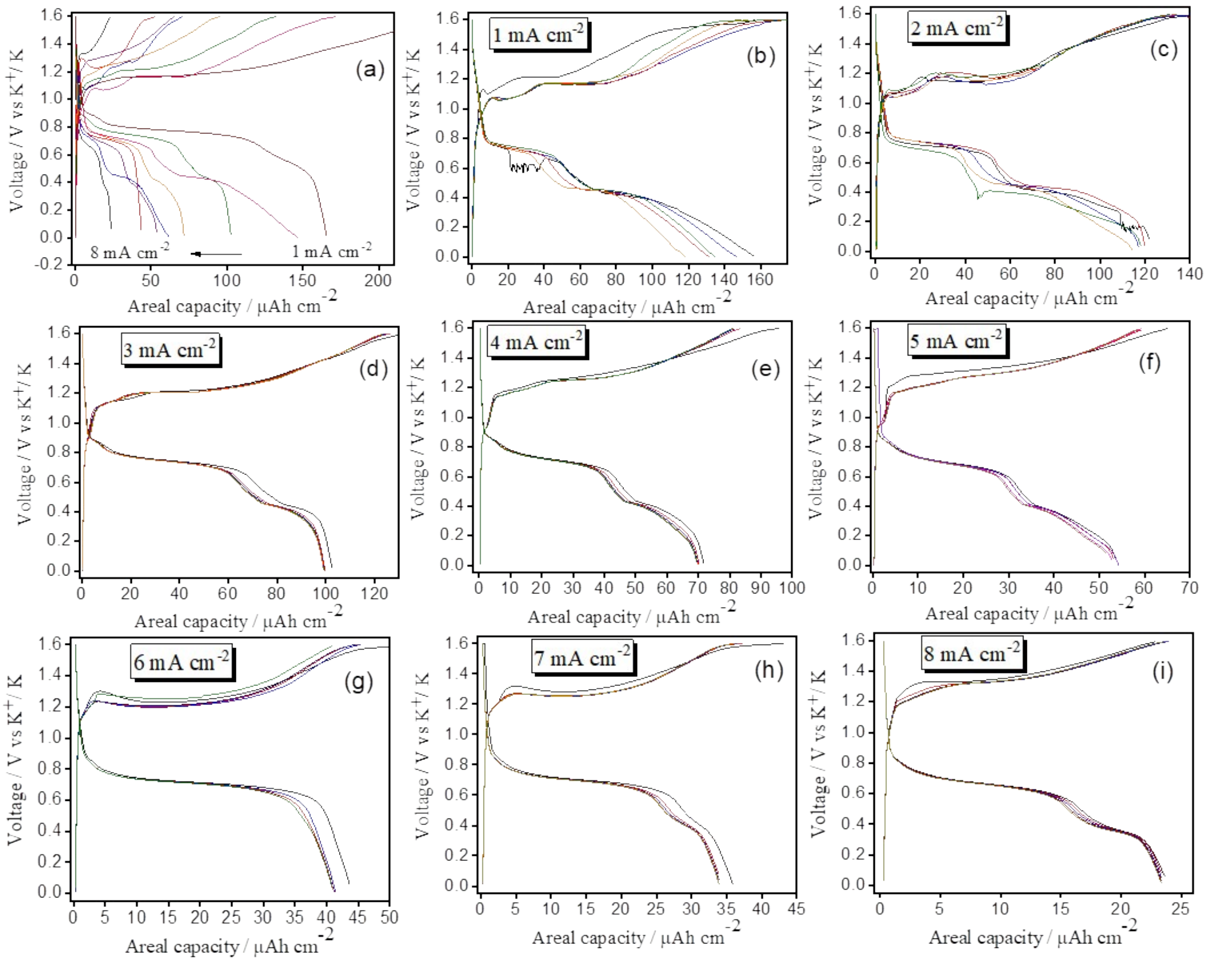

Figure S15: (a) Areal capacity profile of FeS (cell A650) device with respect to current density ranges; (b-i) Areal capacity profiles of 5 cycles at current densities from 1 mA $cm^{-2}$to 8 mA cm^{-2}.

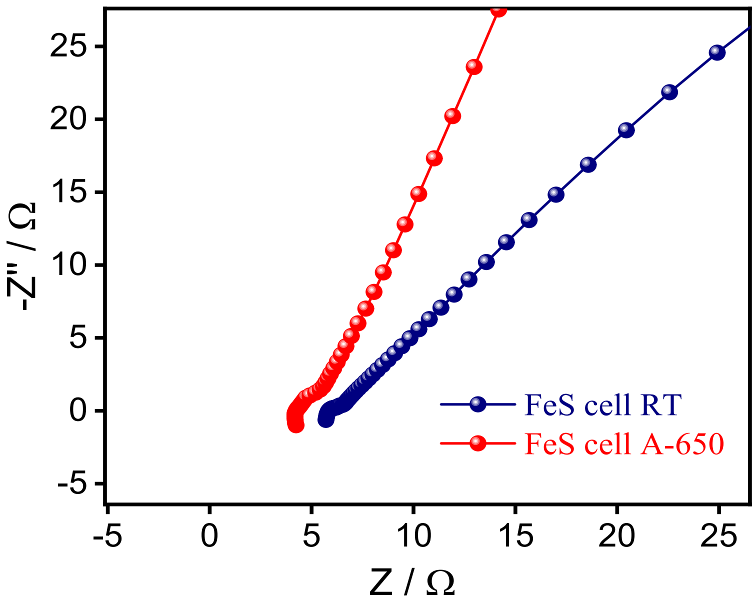

Figure S16: EIS comparison of both thin film supercapacitor devices FeS cell RT and Cell A-650.

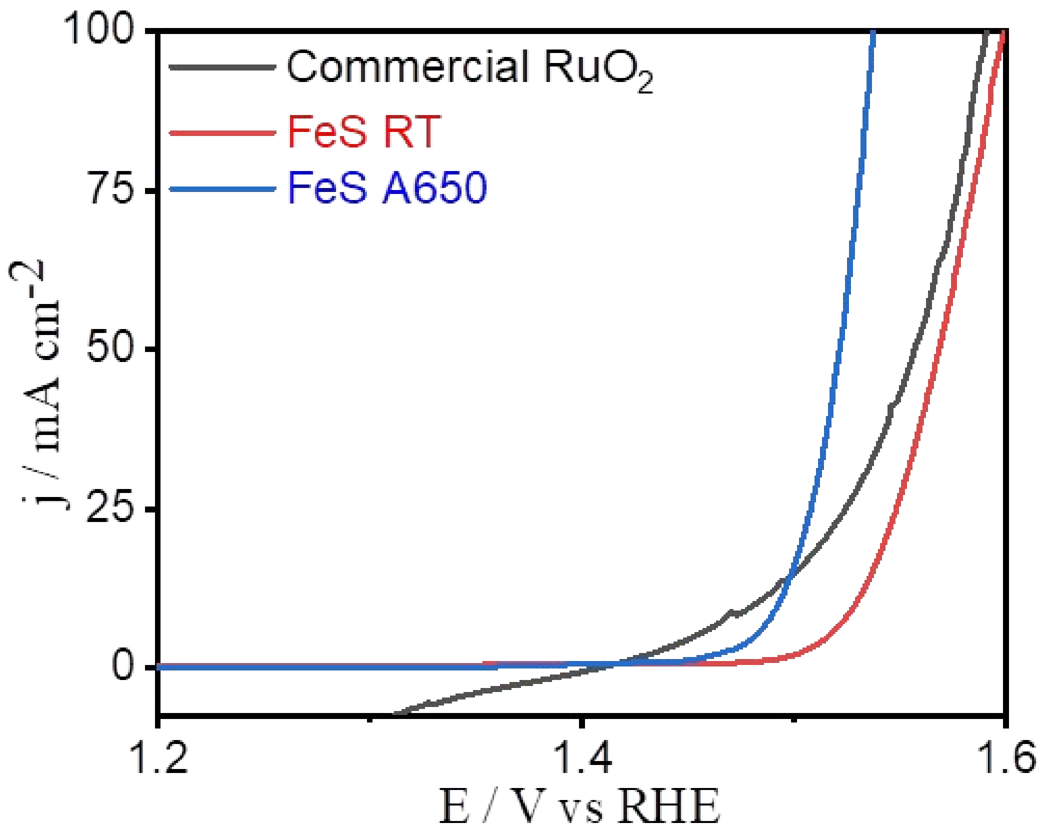

Figure S17: (a) LSV comparison of commercial RuO_2, FeS RT and FeS A650 acquired at 10 mV s^{-1} in an alkaline 1 M KOH medium.

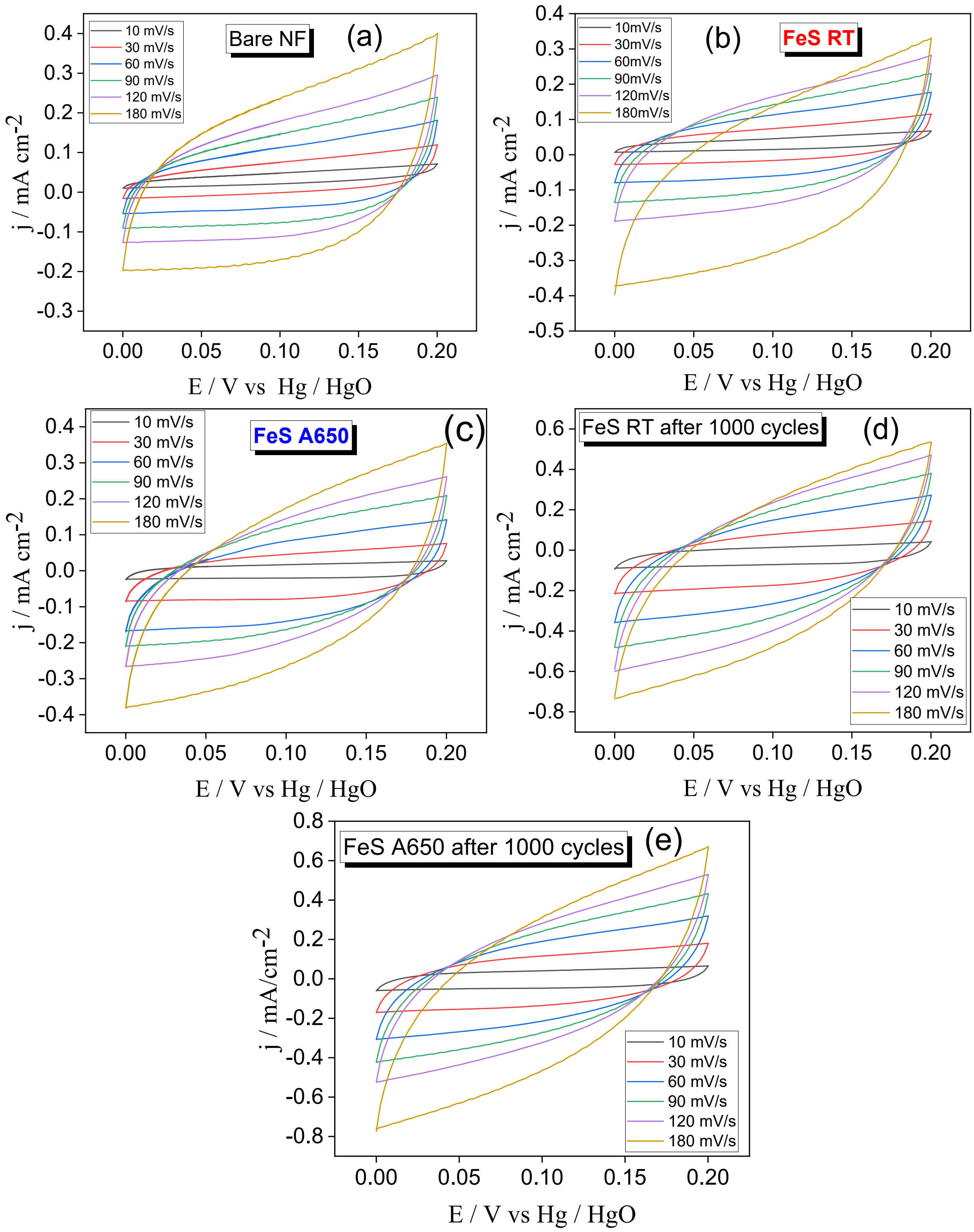

Figure S18: CV curves at various scan rates; (a) Bare NF; (b) FeS RT; (c) Fes A650; (d) FeS RT after 1000 cycles; (e) FeS A650 after 1000 cycles.

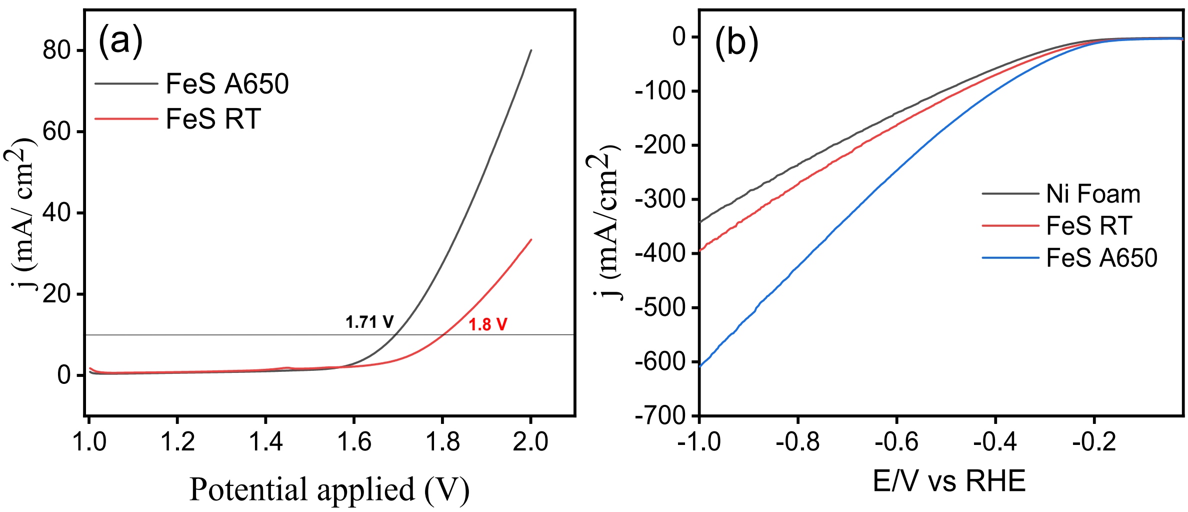

Figure S19: (a) LSV of FeS RT and FeS A650 thin film electrode comparison in O_2 saturated in alkaline 1M KOH medium;(b) LSV curve showing the HER response of bare Ni foam, FeS RT and FeS A650 electrodes in alkaline 1M KOH medium.

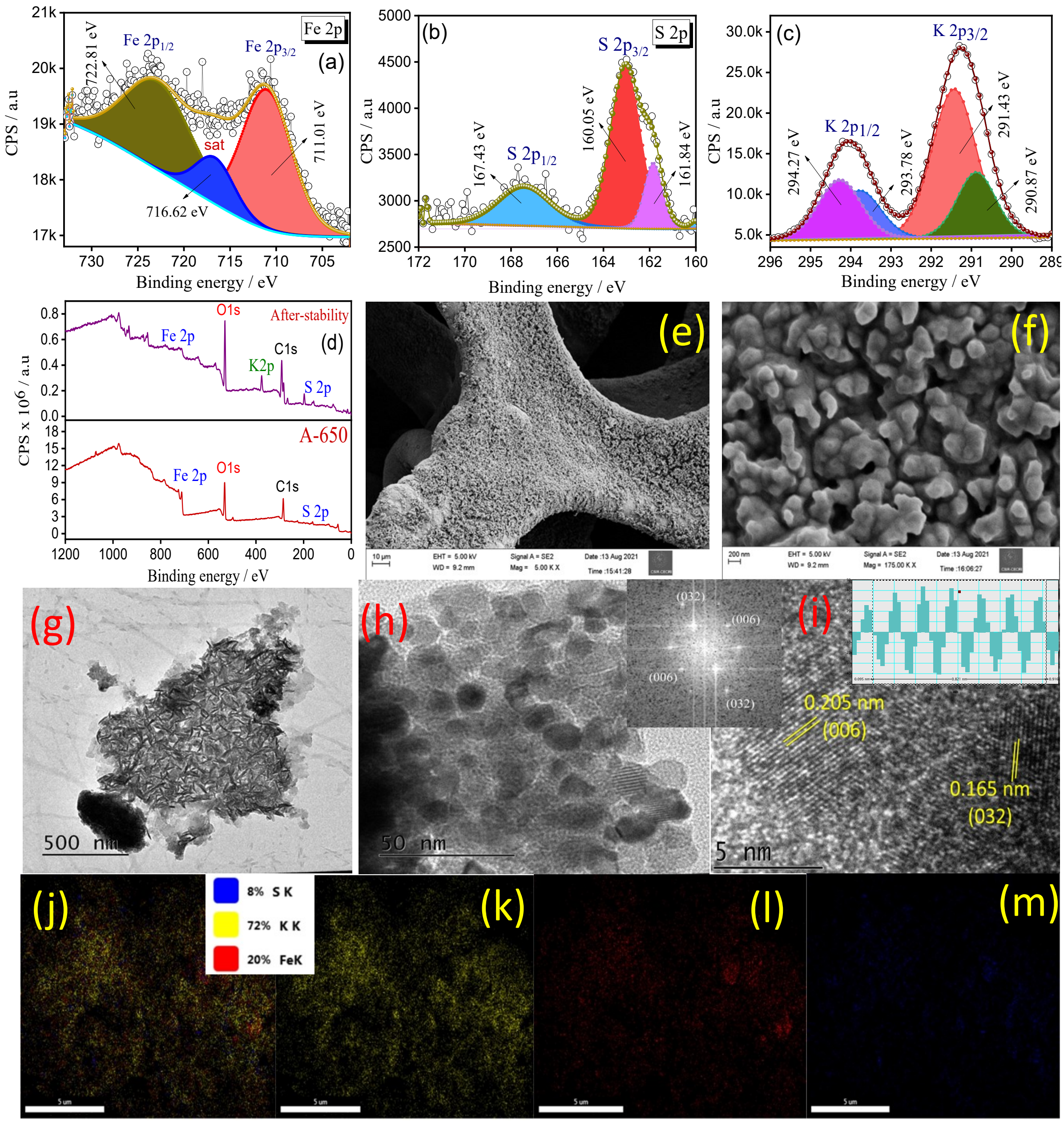

Figure S20: Post study analysis(Ex-situ) of FeS (A650) thin film (a) XPS deconvoluted spectra of Fe 2p; (b)XPS deconvoluted spectra of S 2p; (c) K 2p; (d) Survey spectrum comparision of pristine and after stability; (e& f) FESEM morphologies of FeS thin film after stability at 5 KX and 175 KX; (g& h) TEM morphologies (inset: FFT image); (i) d- spacing (inset: d-spacing profile spectrum); (j-l)HRTEM-EDS mapping for F,S and K.

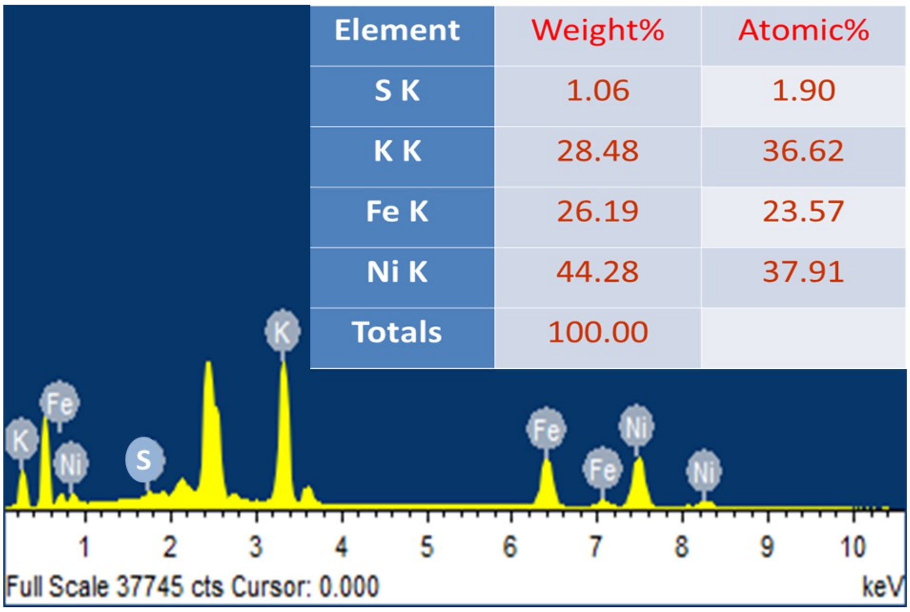

Figure S21: EDAX spectrum of FeS (cell A650) electrode after stability analysis.

Table S1: The electrochemical stability of the volumetric capacitance comparison study of symmetric supercapacitor based reported literature

Material & Configuration	**Method**	**Electrolyte & Voltage window**	**Volumetric capacitance**	**Specific Energy density**	**Specific Power density**	**Stability & Retention**	**Ref**
SWNT)/nitrogen-doped rGO Symmetric	Hydro-thermal synthesis	PVA/H_3PO_4 1.0V	300 F cm^{-3}	6.3 mWh cm^{-3}	1,085 mW cm^{-3}	10,000 93%	20
$Co(OH)_2$/rGO Symmetric	Hydro-thermal synthesis	PVA/KOH 0–1.4 V	39 F cm^{-3}	20 mWh cm^{-3}	56 mW cm^{-3}	2000 99.35%	21
Co_3O_4 Symmetric	E-beam evaporation	LiPON 2 V,	37 (±2) F cm^{-3}	8 (±2) mWh cm^{-3}	16 (±2) W cm^{-3}	30000	22
RGO/Ag/Fe_2O_3 FSS Symmetric	SILAR	PVA-LiCl 1.2V	18.2 F cm^{-3}	3.65 mWh cm^{-3}	290.3 mW cm^{-3}	10000 100%	23
MnO_2/Au NSP Symmetric	Anodization	PVA/H_3PO_4 1.0V	20.35 F cm^{-3}	1.75 mWh cm^{-3}	13.46 W cm^{-3}	5000 87.5%	24
rGO-TiO_2 Symmetric	Vacuum filtration	PVA/KOH 0.8V	237 F cm^{-3}	16 mWh cm^{-3}	1.8 W cm^{-3}	4000	25
MnO_2 spheres Symmetric	Hydro-thermal synthesis	PVA-BMIMCl-Li_2SO_4 1.5V	81 F cm^{-3}	6.6 mWh cm^{-3}	549 mW cm^{-3}	6000 91.5%	26
FeS Symmetry	**PLD**	**PVA-KOH 1.6 V**	**841 F cm^{-3}**	**14.95 mWh cm^3**	**6.4 W cm^{-3}**	**14000 90%**	**This work**

Table S2: The electrochemical stability of the areal capacitance comparison study of symmetric supercapacitor based reported literature

Materials& Configuration	**Method**	**Voltage window & Electrolyte**	**Specific capacitance (Areal)**	**Stability**	**Ref**
CrN Symmetric	DC magnetron sputtering	0.5 M H_2SO_4 0.8V	12.8 mF cm^{-2}	20 000 92.1%	27
V_2O_5 Symmetric	Thermal Evaporation	PVA-KOH 1.0V	9.7 mF cm^{-2}	30000 95%	28
VN Symmetric	Chemical Solution Deposition (CSD)	1 M KOH 0.8 V	60 mF cm^{-2}	15,000 91.2%	29
$Ni(OH)_2$ Symmetric	Electro-deposition	6 M KOH 0.4V	235 mF cm^{-2}	20,000 -----	30
KF@PPy/*f*-CNT Symmetric	Synthesis	PVA/H_2SO_4 - 0.2 to +0.8 V	258 mF cm-2	2500 97.4%	31
FeOOH@MnO_2 Symmetric	Hydro-thermal Synthesis	PVA-$LiClO_4$ 1.0V	252 mF cm^{-2}	2000 99.5%	32
MoO_3/GO/MWCNTs Symmetric	Electro-deposition	PVA/H_3PO_4 2.5 V	103 mF cm^{-2}	2000 86.8%	33
PPy:PSS Symmetric	Co-precipitation method	1 M KOH 0 to 1.0 V	175.3 mF cm^{-2}	5000 86.3%	34
V_2O_5 Symmetric	sol-gel	$BMIMBF_4$ - $LiClO_4$ 2.0 to þ2.0 V	310 mF cm^{-2}	2000 65%	35
MnO_2/CNT Symmetric	Spinning method	CMC-$LiClO_4$ 1.2V	135 mF cm^{-2}	10,000 86%	36
Fe_2O_3 Symmetric	Synthesis	PVA/PAAS/KOH 1.2 V	3.3 mF cm^{-2}	5000 85.6%	37
FeS Symmetric	**PLD**	**PVA-KOH 1.6V**	**420.6 mF cm^{-2}**	**14000 90%**	**This work**

Table S3: State of art of the thin film based electro catalytic materials and their OER performance characteristics with other reported literature

Catalyst	Synthesis Method	Medium	Overpotential @ 10mA cm^{-2}	Tafel (mV/dec)	Substrate	Ref.
A-MnS	Hydrothermal and Anion Exchange	1 M KOH	292 mV	70	Stainless Steel	38
$NiSe_2$@MoS_2	Electrodeposition and Hydrothermal	1 M KOH	267 mV	85	Carbon Fiber Paper	39
MoS_2	Atomic layer Deposition	1 M KOH	273mV	61	Carbon Fiber Paper	40
$Ni_{0.88}Co_{1.22}Se_4$	Two step reflux method	1 M KOH	320mV	78	FTO	41
NiS	Hot Injection Method	1 M KOH	300mV	---	Ni Foam	42
NiS@Ni Foam	Aerosol assisted Chemical Vapor Deposition	1 M KOH	300mV	81.3	Ni Foam	43
Co_9S_8 Holoow Sphere	Solvothermal	1 M KOH	285mV	58	Glassy Carbon	44
$Ni_xCo_{3-x}S_4$	Hot Injection Method	1 M KOH	327mV	89	Ni Foam	45
NiFeCo-S/C	Wet chemical and Annealing	1 M KOH	271mV	45.4	Rotating Disk Glassy carbon	46
Metallic Ni_2S_3 film	Atomic Layer Deposition	1 M KOH	400mV	51	Au on Si/SiO_2	47
$CoFe/(OH)_x$	SILAR	1 M KOH	275mV	34	Copper	48
CoS	Hydrothermal	1 M KOH	383mV	38	Glassy Carbon	49
FeS	**PLD**	**1M KOH**	**263mV**	**48**	**Ni Foam**	**This Work**

References:

[1] Y. W. Lee, B. S. Kim, J. Hong, H. Choi, H. S. Jang, B. Hou, S. Pak, J. Lee, S. H. Lee, S. M. Morris, D. Whang, J. P. Hong, H. S. Shin, S. N. Cha, J. I. Sohn, J. M. Kim, *Nano Energy* **2017**, *37*, 15.

[2] T. M. Higgins, S. Finn, M. Matthiesen, S. Grieger, K. Synnatschke, M. Brohmann, M. Rother, C. Backes, J. Zaumseil, *Adv. Funct. Mater.* **2019**, *29*, DOI 10.1002/adfm.201804387.

[3] N. Li, T. Lv, Y. Yao, H. Li, K. Liu, T. Chen, *J. Mater. Chem. A* **2017**, *5*, 3267.

[4] D. Ranjith Kumar, S. Kesavan, M. L. Baynosa, J. J. Shim, *Appl. Surf. Sci.* **2018**, *448*, 547.

[5] G. Yilmaz, X. Lu, *ChemNanoMat* **2016**, *2*, 719.

[6] C. Yang, N. Hu, W. Wang, B. Cao, *J. Power Sources* **2018**, *399*, 115.

[7] P. Yu, X. Zhao, Z. Huang, Y. Li, Q. Zhang, *J. Mater. Chem. A* **2014**, *2*, 14413.

[8] M. Yao, Y. Chen, Z. Wang, C. Shao, J. Dong, Q. Zhang, L. Zhang, X. Zhao, *Chem. Eng. J.* **2020**, *395*, 124057.

[9] C. Yang, L. Zhang, N. Hu, Z. Yang, Y. Su, S. Xu, M. Li, L. Yao, M. Hong, Y. Zhang, *Chem. Eng. J.* **2017**, *309*, 89.

[10] L. Yao, C. Zhou, N. Hu, J. Hu, M. Hong, L. Zhang, Y. Zhang, *Appl. Surf.*

Sci. **2018**, *435*, 699.

[11] P. Apelgren, M. Amoroso, K. Säljö, M. Montelius, A. Lindahl, L. Stridh Orrhult, , *Mater. Today Proc.* **2019**, *27*, 0.

[12] H. Han, J. S. Lee, S. Cho, *Polymers (Basel).* **2019**, *11*, 3.

[13] Y. Tian, C. Yang, W. Que, X. Liu, X. Yin, L. B. Kong, *J. Power Sources* **2017**, *359*, 332.

[14] Y. Bu, M. Cao, Y. Jiang, L. Gao, Z. Shi, X. Xiao, M. Wang, G. Yang, Y. Zhou, Y. Shen, *Electrochim. Acta* **2018**, *271*, 624.

[15] X. Wang, H. Huang, F. Zhou, P. Das, P. Wen, S. Zheng, P. Lu, Y. Yu, Z. S. Wu, *Nano Energy* **2021**, *82*, 105688.

[16] M. A. Spencer, O. Yildiz, I. Kamboj, P. D. Bradford, V. Augustyn, *Energy and Fuels* **2021**, *35*, 16183.

[17] X. Li, T. Gao, Q. Liu, Y. Xu, J. Li, D. Xiao, *Mater. Chem. Front.* **2021**, *5*, 3636.

[18] J. K. Kim, J. Scheers, H. S. Ryu, J. H. Ahn, T. H. Nam, K. W. Kim, H. J. Ahn, G. B. Cho, P. Jacobsson, *J. Mater. Chem. A* **2014**, *2*, 1774.

[19] K. Song, X. Wang, J. Wang, B. Zhang, C. Zuo, *ChemElectroChem* **2018**, *5*, 1297.

[20] D. Yu, K. Goh, H. Wang, L. Wei, W. Jiang, Q. Zhang, L. Dai, Y. Chen,

Nat. Nanotechnol. **2014**, *9*, 555.

[21] Y. Rong, Y. Chen, J. Zheng, Y. Zhao, Q. Li, *J. Colloid Interface Sci.* **2021**, *598*,

[22] T. Göhlert, P. F. Siles, T. Päßler, R. Sommer, S. Baunack, S. Oswald, O. G. Schmidt, *Nano Energy* **2017**, *33*, 387.

[23] Z. Zou, W. Xiao, Y. Zhang, H. Yu, W. Zhou, *Appl. Surf. Sci.* **2020**, *500*, 144244.

[24] Y. Gao, H. Jin, Q. Lin, X. Li, M. M. Tavakoli, S. F. Leung, W. M. Tang, L. Zhou, H. L. Wa Chan, Z. Fan, *J. Mater. Chem. A* **2015**, *3*, 10199.

[25] J. Du, C. Zheng, W. Lv, Y. Deng, Z. Pan, F. Kang, Q. H. Yang, *Adv. Mater. Interfaces* **2017**, *4*, 1.

[26] J. Zhi, O. Reiser, Y. Wang, A. Hu, *Nanoscale* **2016**, *8*, 11976.

[27] B. Wei, H. Liang, D. Zhang, Z. Wu, Z. Qi, Z. Wang, *J. Mater. Chem. A* **2017**, *5*, 2844.

[28] R. Velmurugan, J. Premkumar, R. Pitchai, M. Ulaganathan, B. Subramanian, *ACS Sustain. Chem. Eng.* **2019**, *7*, 13115.

[29] Z. Q. Wu, B. B. Yang, H. Li, H. Y. Tong, X. Wang, C. D. Li, L. L. Zhu, R. H. Wei, L. Hu, C. H. Liang, X. B. Zhu, Y. P. Sun, *J. Power Sources* **2021**, *507*, DOI 10.1016/j.jpowsour.2021.230269.

[30] A. Pimsawat, A. Tangtrakarn, N. Pimsawat, S. Daengsakul, *Sci. Rep.* **2019**, *9*, 1.

[31] J. P. Jyothibasu, R. H. Lee, *Polymers (Basel).* **2018**, *10*, 6.

[32] R. B. Pujari, S. J. Patil, J. Park, A. Shanmugasundaram, D. W. Lee, *J. Power Sources* **2019**, *436*, 226826.

[33] M. Faraji, A. Abedini, *Int. J. Hydrogen Energy* **2019**, *44*, 2741.

[34] X. Jing, Y. Zhang, H. Jiang, Y. Cheng, N. Xing, C. Meng, *J. Alloys Compd.* **2018**, *763*, 180.

[35] F. Azadian, A. C. Rastogi, *Electrochim. Acta* **2020**, *330*, 135339.

[36] B. Patil, S. Ahn, C. Park, H. Song, Y. Jeong, H. Ahn, *Energy* **2018**, *142*, 608.

[37] S. Peng, L. Yu, P. Kakvand, M. S. Rahmanifar, G. Zhang, M. Kong, J. Zhu, S. Tang, R. Ren, M. S. Faber, Z. Li, X. Yu, F. Su, M. Miao, **n.d.**

[38] R. B. Pujari, G. S. Gund, S. J. Patil, H. S. Park, D. W. Lee, *J. Mater. Chem. A* **2020**, *8*, 3901.

[39] S. Liu, B. Li, S. V. Mohite, P. Devaraji, L. Mao, R. Xing, *Int. J. Hydrogen Energy* **2020**, *45*, 29929.

[40] S. Materials, S. D. B. K. Sharma, A. Stoesser, S. K. Mondal, S. K. Garlapati, M. H. Faway, V. S. K.Chakravadhanula, R. Kruk, H. Hahn,

ACS Appl. Mater. Interfaces **2018**, *10*, 0.

[41] D. V. Shinde, L. De Trizio, Z. Dang, M. Prato, R. Gaspari, L. Manna, *Chem. Mater.* **2017**, *29*, 7032.

[42] G. E. Ayom, M. D. Khan, T. Ingsel, W. Lin, R. K. Gupta, S. J. Zamisa, W. E. van Zyl, N. Revaprasadu, *Chem. - A Eur. J.* **2020**, *26*, 2693.

[43] M. A. Ehsan, A. Rehman, A. Afzal, A. Ali, A. S. Hakeem, U. A. Akbar, N. Iqbal, *Energy and Fuels* **2021**, *35*, 16054.

[44] X. Feng, Q. Jiao, T. Liu, Q. Li, M. Yin, Y. Zhao, H. Li, C. Feng, W. Zhou, *ACS Sustain. Chem. Eng.* **2018**, *6*, 1863.

[45] C. Gervas, M. D. Khan, C. Zhang, C. Zhao, R. K. Gupta, E. Carleschi, B. P. Doyle, N. Revaprasadu, *RSC Adv.* **2018**, *8*, 24049.

[46] M. H. Han, M. W. Pin, J. H. Koh, J. H. Park, J. Kim, B. K. Min, W. H. Lee, H. S. Oh, *J. Mater. Chem. A* **2021**, *9*, 27034.

[47] T. A. Ho, C. Bae, H. Nam, E. Kim, S. Y. Lee, J. H. Park, H. Shin, *ACS Appl. Mater. Interfaces* **2018**, *10*, 12807.

[48] S. Liu, B. Liu, C. Gong, Z. Li, *Appl. Surf. Sci.* **2019**, *478*, 615.

[49] W. Adamson, C. Jia, Y. Li, C. Zhao, *Electrochim. Acta* **2020**, *355*, 136802.